Molecular Dynamics Study of Two-Component Systems: The Shape and Surface Structure of Water/Ethanol Droplets

Mounir Tarek and Michael L. Klein*

Center for Molecular Modeling, Department of Chemistry, University of Pennsylvania, Philadelphia, Pennsylvania 19104-6323

Received: July 14, 1997; In Final Form: September 5, 1997[⊗]

Molecular dynamics simulations have been performed at $T = 260$ K on three different sized ethanol/water droplets with a mole fraction of ethanol $x = 12\%$. The calculations were initiated from near spherical configurations taken from simulations of the bulk mixture with the same composition. The results are discussed in comparison to the microphysical models used in nucleation theories. For the droplet having a comparable size to the so-called "critical" cluster, all the ethanol molecules repartition to the surface. The shapes and surface structure of the droplets have been characterized and exhibit increasing fluctuations with decreasing size. These two observations may help explain the present discrepancy between the predicted and calculated rates of nucleation for ethanol/water droplets.

Introduction

Due to implications in atmospheric and environmental sciences, the nucleation of liquid-phase binary mixtures from the vapor continues to attract attention.[1] The development of experimental techniques is allowing accurate measurements of the rates of nucleation,[2−5] and two theoretical approaches have been proposed to predict that rate. The first approach is based on density functional theory and utilizes Monte Carlo or molecular dynamics computer simulations to calculate the free energies of the droplets. Due to computational limitations, the approach has been applied only to Lennard Jones fluid mixtures.[6] The second "classical" approach, which will be of interest here, is based on the so-called capillary approximation. Here, the droplets are described as spherical objects with a definite composition and their thermodynamic properties (volume, surface tension, etc.) are used to derive the nucleation rate for a given system.

Historically, the use of the classical homogeneous theory[7] has successfully predicted critical activities of a number of pure systems and binary mixtures.[8] However, very poor agreement with experiment has been found for nonideal mixtures.[2,3,9,10] It was first Renninger et al.[11] and then Wilemski[12,13] who, in the early 1980s, showed that the classical theory was inconsistent when the surface tension of the system changes significantly with composition. Wilemski proposed a "revised classical theory" using the Gibbs adsorption equation, which takes into account surface-enrichment effects. Flageollet-Daniel et al.[14] later noted that the surface-tension values taken from macroscopic systems (flat surfaces) are not appropriate for critical size droplets, since the average concentration in the bulk is highly dependent on the number of molecules in the surface.

In general, even though the surface tension is a function of the surface composition microscopically, it is often related to the bulk composition that is used in the reported macroscopic measurements. For consistency and to be able to use measurable surface tensions, Flageollet-Daniel et al. introduced a lattice model that allows one to relate the bulk concentration to the surface concentration in the critical nucleus. In this model, the surface tension of the system is expressed as a function of the pure components surface tensions, their volume fractions, and three adjustable parameters. The experimental (macroscopic) surface-tension values for the corresponding system are used to calculate the surface and bulk mole fractions in the droplet.

Using a similar approach, Laaksonen[15] introduced an explicit cluster model containing no parameters. The droplet, assumed spherical, is composed of an interior bulk and a unimolecular surface layer. The molecular areas are assumed independent of composition but dependent on the surface curvature. A semiempirical equation defining the surface tension of the system as a function of the molecular volumes and surface tension of the pure components is used. The fit of this equation using the experimental surface tension values allows one to get the surface and bulk mole fractions.

Alcohol/water mixtures are probably the most commonly studied systems, and both models have been tested for these systems. In both cases, the comparison with critical supersaturations (activities) was claimed to be good. However, it is only recently that Strey et al.[5,16,17] have been able to determine, from nucleation rate measurements, the composition of the critical cluster for a variety of mixtures. The authors show that the slope of the nucleation rate surface allows the specification of the number of molecules in the droplet, independent of a particular model. The comparison of their experimental results to the predictions by the cluster theory revealed an overall qualitative agreement. Quantitatively, the nucleation rates estimated were found to be 3−6 orders of magnitude higher than the experimental ones and the critical clusters smaller.

The recent results of Strey et al.[16,17] will likely stimulate research into more sophisticated models for binary nucleation droplets and/or refinement of the existing ones. However, in the absence of a description of the critical nuclei at the molecular level, it is likely that these models will always be based on "classical" descriptions.

The aim of this paper is to provide insight into the molecular surface structure of related binary nuclei through molecular dynamics simulations, namely an ethanol/water cluster, and to study their shape properties as a function of their size. Anticipating our results, we will see that the distribution of the molecules in the cluster having a comparable size to the critical nucleating droplets is not in agreement with the predictions of the existing nucleation theories.

[⊗] Abstract published in *Advance ACS Abstracts,* October 15, 1997.

S1089-5639(97)02278-0 CCC: $14.00

TABLE 1: Details of the MD Simulations[a]

system	N_w	N_e	run length (ps)
large	415	60	1200
medium	144	19	780
small	53	7	960

[a] N_w and N_e are, respectively, the number of water and ethanol molecules in the droplet.

Potential Model and MD Simulations

The intermolecular potential employed in the present work is similar to that used in the previous study of the ethanol−water mixtures.[18] The rigid three-site SPC/E model of Berendsen et al. was used for water.[19] The potential for ethanol was essentially the pseudoatom model (i.e., methylene and methyl groups are represented by single sites) of Jorgensen,[20] except that it was made flexible in the present work by adding harmonic bond stretching and bond angle bending. The parameters for the intermolecular ethanol−water Lennard−Jones interactions were obtained by using the Lorentz−Bertholot mixing rules.[20]

The molecular dynamics simulations were carried out for three different droplet sizes starting from mixtures around 12% ethanol molar fraction. (see Table 1 for details). At this concentration range, there is a substantial reduction of the surface tension of the solution and the system is still at the water-rich region. One expects that the ethanol molecules will aggregate at the surface of the droplets.

The initial configurations were set up starting from well-equilibrated bulk water configurations, and the appropriate number of water molecules (chosen randomly) were replaced by ethanol molecules. Following energy minimization of the solution, MD (molecular dynamics) simulations were carried out with three-dimensional periodic boundary conditions for 15 ps at constant temperature ($T = 298$ K) and 70 ps at constant temperature and pressure ($P = 0$), during which time the densities converged near the experimental value.[22] The final configurations of the constant-pressure runs were used to initiate the simulations of the droplets. The three clusters of interest were generated from the bulk mixture by selecting all molecules lying within a cutoff radius of 16, 11, and 8 Å, respectively. The resulting droplets, which were then placed in a much larger constant-volume simulation box, (see Table 1 for details), were used to initiate MD simulations at constant temperature. The equations of motion were integrated using a Verlet-like algorithm[21] with a time step of time of 1.5 fs. Temperature control was affected by using the Nosé−Hoover chain method[23] with thermostat time scales of 0.5 ps. Bonds involving hydrogen atoms were constrained using the SHAKE algorithm.[24] No periodic boundary conditions were used, and the nonbonded interactions were computed for all pairs of atoms in the system. At the temperature studied ($T = 260$ K), no evaporation of water molecules was observed during the length of the MD simulations, which spanned approximately a nanosecond.

Results and Discussion

Radial density profiles of the water and ethanol molecules averaged over the simulation runs are displayed in Figure 1. These plots show, as expected, an ethanol excess at the surface. For the largest droplet the situation is similar to that found previously for a planar interface (at the same average concentration):[18] a depletion layer beneath the interface is formed. The shape of the density profiles close to the center ($R \leq 4$ Å) is subject to large statistical errors due to the small size of the volume element over which the density is calculated.

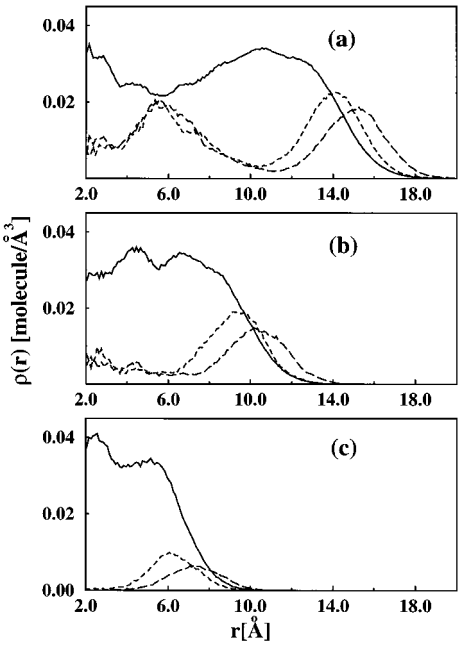

Figure 1. Number density profiles for water (solid line) the and carbon (dashed lines) and oxygen (dotted lines) atoms of ethanol averaged over the simulation: (a) large, (b) midsize, and (c) small droplet, respectively. For clarity, the ethanol atom densities have been scaled by a factor of 4.

The staggering of the ethanol oxygen and terminal methyl group density profiles indicates that molecules in the outer shell of the cluster orient themselves with the hydrophobic tail pointing radially out of the interface, while inside the cluster core no preferred orientation is obtained for the alcohol molecules.

For the smaller clusters, Figure 1 shows an ethanol enrichment at the surface as well. However, inside the droplets the concentration of solute molecules drops gradually as the size of the cluster decreases. For the smallest droplet, all of the ethanol molecules aggregate at the surface. A quantitative description of the droplets, in terms of average radius and surface area per molecule, is difficult since their shapes are no longer spherical, as seen in the snapshots displayed in Figure 2. This departure from the spherical shape explains the broadening of the density-profile distributions of the interfacial water and ethanol as the cluster size decreases.

To characterize droplet shape fluctuations, we analyzed the variation of the inertia tensor of the droplet during the run. The inertia moments I_1, I_2, and I_3 corresponding to the principal axes have been calculated taking into account all the atoms in the cluster. The ratio $R1 = I_2/I_1$ and $R2 = I_3/I_1$, respectively, are displayed in Figure 3. They indicate a pronounced departure from sphericity ($R \simeq 1$) for decreasing size droplets. The general trend observed from Figure 3 is that the fluctuations in shape have the largest amplitudes and smallest frequencies on going from the largest to the smallest cluster.

The time scale for the droplet shape fluctuations has been estimated from the initial decay of $C_e(\epsilon)$, the time autocorrelation function of e, the eccentricity, where

$$C_e(t) = <\delta e(t)\delta e(0)>/<\delta e(0)\delta e(0)> \qquad (1)$$

$\delta e(t) = e(t) - <e(t)>$ and $e = 1 - I_1/I_{av}$, I_{av} being the average inertia moment. The calculated characteristic times τ_e are 120, 30, and 30 ps in order of decreasing droplet size. From the R plots (Figure 3), we see that during these fluctuations, the droplets occasionally adopt a nearly spherical configuration. At

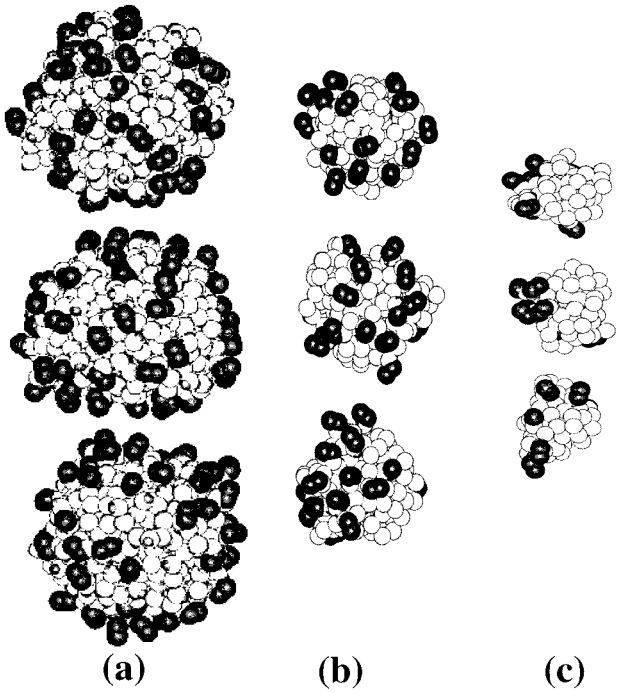

Figure 2. Snapshots of the simulation systems: (a) large, (b) midsize, and (c) small droplet, respectively. From top to bottom, the snapshots are 100 ps apart and are taken from the last 300 ps of the MD trajectories. The oxygen (white), hydrogen (grey), and carbon (black) atoms are drawn as spheres with their corresponding van der Waals radii.

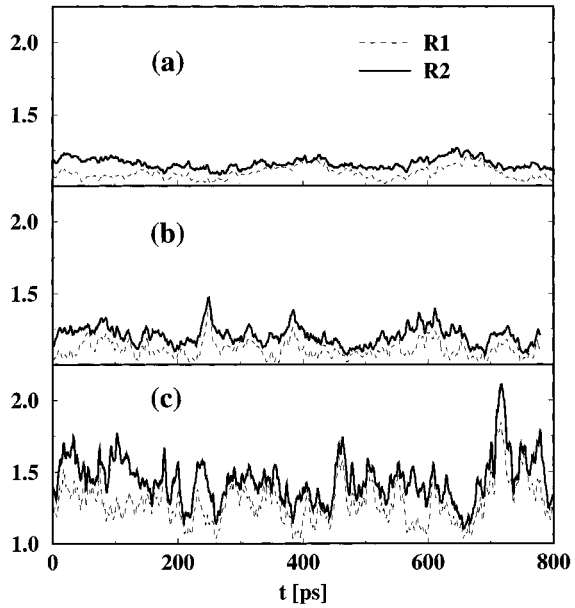

Figure 3. Ratios of the principal inertia moments $R1$ and $R2$ as a function of time: (a) large, (b) midsize, and (c) small droplet, respectively. where $R = 1$ denotes a spherical droplet shape. Note the increased amplitude and frequency of the fluctuations in the small droplet.

such times, we have estimated the average volume V of the droplet ($V = {}^4/_3\pi\langle R_s^3\rangle$) and the average surface area per ethanol molecule $S = 4\pi\langle R_s^2\rangle/N_s$, where $\langle R_s\rangle$ is the average position of the surface ethanol oxygen atoms at each time step. The results, reported in Figure 4 along with the value for the flat (infinite radius of curvature) surface,[25] indicate that the surface area per ethanol molecule is linearly increasing with droplet curvature.

The results presented in this paper have characterized aspects of the structure and the dynamics of small droplets of binary

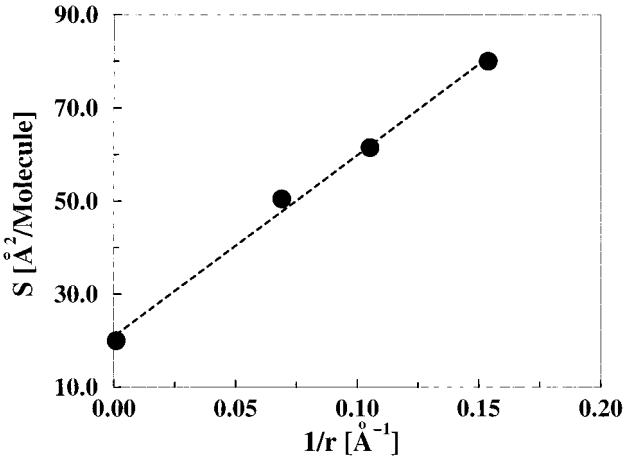

Figure 4. Surface area per ethanol molecule as a function of r, the radius of the droplet, which is estimated at the time when the clusters instantaneously have a spherical shape.

mixtures. The major points revealed by analysis of the molecular dynamics simulation trajectories are the repartition of molecules inside the droplet and the overall shape and structure. The study of three systems going from a large droplet (closest to a macroscopic flat-surface situation) to a droplet the size claimed for a critical cluster[16] shows that the expected surface enrichment of such clusters significantly changes the concentration of the interior bulk. The surface area per surfactant molecule increases with an increase in the droplet curvature, and the shape of the cluster seems to deviate increasingly from spherical shape.

While the study of different sized droplets permits us to investigate the general properties of small clusters, it is the smallest cluster that relates directly to nucleation phenomena. The Gibbs free energy of cluster formation is $\Delta G = n_1\Delta\mu_1 + n_2\Delta\mu_2 + A\gamma$, where n_i and μ_i are the number of molecules and chemical potential of the species i, A the surface area of the cluster, and γ its surface tension. The nucleation rate J is usually expressed in terms of ΔG^*, the free energy required to form a mixed critical nucleus from the vapor phase, as $J = C\exp(-\Delta G^*/kT)$, where ΔG^* is a function of the surface tension γ and the molar volume of the droplet, namely $\Delta G^* = (4\pi/3)r^{*2}\gamma$. The constant C is known to be a slowly varying function and hence, a good prediction of the nucleation rate depends on the estimation of the surface tension and the volume of the droplet. As briefly described in the Introduction, the lattice and cluster models are used to estimate the surface tension. They take into account the surface enrichment and the effect of the finite cluster size on the bulk concentration. However, quantitatively, none of the models agrees with our finding that in a cluster of small size, all the surfactant molecules may be at the surface.

In addition, the present study has shown that the small size clusters can depart severely from a spherical shape. The characteristic times observed for the shape fluctuations appear to be in the range of neutron and light scattering experiments and, hence, could perhaps be directly probed. These shape fluctuations are very similar to those characterizing the structure of spherical micelles in solution,[26] and it is likely that considering a "critical" size cluster with a fixed shape is a poor approximation. A valid description of the nucleation phenomena should probably take into account the contributions of these fluctuations to the surface free energy.[27]

The present results are naturally limited by the quality of the potential parameter used. In a previous study of an ethanol/water flat interface,[18] it was shown that the calculated surface

tension was overestimated by about 50% compared to the experimental value[28] for a system at the same concentration. The simulation system corresponds to a state characteristic of a lower ethanol concentration. The potentials employed herein yield an ethanol excess consistent with that measured for a solution at the same surface tension. Also, the structure of the interface (thickness) was in agreement with neutron results.[29] In the present MD simulation, it is not clear how to calculate the surface pressure for these small fluctuating objects, which precludes unambiguous comparison to theories of nucleating droplets. Nonetheless, the study presented here constitutes a qualitative contribution toward the understanding of the structure and properties of nanoscale binary droplets such as those involved in nucleation. The calculation suggests possible reasons for the current discrepancy between nucleation rates predicted by explicit "molecular" models of critical clusters and experiments. The present study suggests that additional studies over a wide range of concentrations based on improved interactions potentials would likely be informative.

Acknowledgment. This research was supported by generous grants from Procter & Gamble and the National Science Foundation. The simulations benefited from facilities provided by Grant No. NSF DMR 96-32598. The authors are grateful to R. Strey and D. J. Tobias for helpful discussions.

References and Notes

(1) Strey, R.; Wagner, P. E.; Viisanen, Y. In *Nucleation and Atmospheric Aerosols*; Fukuta, N., Wagner, P. E., Eds.; Deepack: Hampton, 1992.; Reiss, H. In *Nucleation*; Zettelmoyer, A. C., Elsevier: New York, 1977. Mirabel, P. J.; Jaecker-Voirol, A. In *Atmospheric Aerosols and Nucleation*; Wagner, P. E., Vali, G., Eds.; Springer: Berlin, 1988.

(2) Mirabel, P.; Katz, J. L. *J. Chem. Phys.* **1977**, *67*, 1697.

(3) Zahoransky, R. A.; Peters, F. *J. Chem. Phys.* **1985**, *83*, 6425.

(4) Schmitt, J. L.; Whitten, J.; Adams G. W.; Zalabasky, R. A. *J. Chem. Phys.* **1990**, *92*, 3693. Whimpfheimer, T.; Chowdhury, M. A.; Reiss, H. *J. Phys. Chem.* **1992**, *97*, 716.

(5) Strey, R.; Viisanen, Y. *J. Chem. Phys.* **1993**, *99*, 4693.

(6) Oxtoby, D. W.; Evans, R. *J. Chem. Phys.* **1988**, *89*, 7521. Zeng, X. C.; Oxtoby, D. W. *J. Chem. Phys.* **1991**, *94*, 4472. Zeng, X. C.; Oxtoby, D. W. *J. Chem. Phys.* **1991**, *95*, 5940.

(7) Reiss, H. *J. Chem. Phys.* **1950**, *18*, 840.

(8) Katz, J. L. *J. Chem. Phys.* **1970**, *52*, 4733. Katz, J. L.; Scoppa, C. J.; Kumar, N. J.; Mirabel, P. *J. Chem. Phys.* **1975**, *62*, 448. Katz, J. L.; Mirabel, P.; Scoppa, C. J.; Virkler, T. J. *J. Chem. Phys.* **1976**, *65*, 382. Kacker, A.; Heist, R. H. *J. Chem. Phys.* **1985**, *82*, 2734.

(9) Wilemski, G. *J. Chem. Phys.* **1975**, *62*, 3763.

(10) Flageollet, C.; Cao, M. D.; Mirabel, P. *J. Chem. Phys.* **1980**, *72*, 544.

(11) Renninger, R. G.; Hiller, F. C.; Bone, R. C. *J. Chem. Phys.* **1981**, *75*, 1584.

(12) Wilemski, G. *J. Chem. Phys.* **1984**, *80*, 1370.

(13) Wilemski, G. *J. Phys. Chem.* **1987**, *91*, 2492.

(14) Flageollet-Daniel, C.; Garnier, J. P.; Mirabel P. *J. Chem. Phys.* **1983**, *78*, 2600.

(15) Laaksonen, A.; Kulmala, M. *J. Chem. Phys.* **1991**, *95*, 6745. Laaksonen, A. *J. Chem. Phys.* **1992**, *97*, 1983.

(16) Viisanen, Y.; Strey, R.; Laaksonen, A.; Kulmala, M. *J. Chem. Phys.* **1994**, *100*, 6062.

(17) Strey, R.; Viisanen, Y.; Wagner, P. E. *J. Chem. Phys.* **1995**, *103*, 4333.

(18) Tarek, M.; Tobias, D. J.; Klein, M. L. *J. Chem. Soc., Faraday Trans.* **1996**, *92*, 559.

(19) Berendsen, H. J. C.; Grigera, J. R.; Straatsma, T. P. *J. Phys. Chem.* **1987**, *91*, 6269.

(20) Jorgensen, W. L. *J. Phys. Chem.* **1986**, *90*, 1276.

(21) Allen, M. P.; Tildesley, D. J. *Computer Simulation of Liquids*; Oxford University Press: New York, 1989.

(22) Timmermans, J. *Physico-Chemical Constants of Binary Systems in Concentrated Solutions*; Interscience: New York, 1960.

(23) Martyna, G. J.; Tuckerman, M. E.; Klein, M. L. *J. Chem. Phys.* **1992**, *97*, 2635.

(24) Ciccotti, G.; Ryckaert, J. P. *Comput. Phys. Rep.* **1986**, *4*, 345.

(25) Guggenheim, E. A. *Thermodynamics*; North-Holland: Amsterdam, 1967.

(26) Woods, M. C.; Haile, J. M.; O'Connell, J. P. *J. Phys. Chem.* **1986**, *90*, 1875. Brown, D.; Clarke, J. H. *J. Phys. Chem.* **1988**, *92*, 2881. Watanabe, K.; Klein, M. L. *J. Phys. Chem.* **1989**, *93*, 6897.

(27) Ljunggren, S.; Erikson, J. C. *J. Chem. Soc., Faraday Trans. 2* **1984**, *80*, 489.

(28) Butler, J. A. V.; Wightman, A. *J. Chem. Soc.* **1932**, 2089.

(29) Li, Z. X.; Lu, J. R.; Styrkas, D. A.; Thomas, R. K.; Rennie, A. R.; Penfold, J. *Mol. Phys.* **1993**, *80*, 925.